Contact Area Measurements Reveal Loading-History Dependence of Static Friction

S. M. Rubinstein, G. Cohen, and J. Fineberg

The Racah Institute of Physics, The Hebrew University of Jerusalem, Jerusalem 91904, Israel

(Received 31 January 2006; revised manuscript received 30 March 2006; published 30 June 2006)

We perform quantitative measurements of the actual area of contact, A, formed by two rough solids that are subjected to different normal loading protocols. We show that microscopic motion, induced by Poisson contraction or expansion, produces a strong memory dependence of A on the loading history with a large corresponding influence on the system's frictional strength. These effects, together with accompanying transient dynamics, are independent of humidity, loading rates, and material contrast across the interface.

DOI: 10.1103/PhysRevLett.96.256103 PACS numbers: 68.35.Np, 46.55.+d, 81.40.Pq

The dynamics of frictional contacts have been the subject of intensive study for hundreds of years, but many key aspects of friction are still far from understood [1]. We show that one of these, the "static" coefficient of friction, undergoes surprising dynamics.

Consider two blocks of material in contact. Although the interface separating these two blocks is ostensibly planar, it is composed of a multitude of interconnecting point contacts [2] (asperities). The classical Amontons-Coulomb law states that the frictional force at the onset of motion, F_S is independent of the *nominal* contact area. This results from the frictional properties of a system being governed by the asperities' *actual* area of contact [3], A. The value of A, which is generally orders of magnitude less than the nominal contact area [3,4], is dynamic and governed by the local pressure felt at the contacts. In the Bowden and Tabor [3] picture of friction, an applied normal force, F_N, creates local pressure, F_N/A, which is limited by the material's yield stress, σ_y. Thus, an increase in F_N causes a proportional increase of A due to plastic deformation and flow. This proportionality remains in more refined theories of contact, which account for the self-affine nature of the contact surfaces [5,6].

Frictional strength has also been shown to evolve logarithmically with time [3,7,8]. This temporal "aging" has been attributed to either plastic flow for high values of F_N, or effects such as the formation of liquid bridges [9] for lower values of F_N.

Despite its obvious importance, few direct measurements of A have been performed. We perform real-time measurements of A and show that, in response to cyclic changes in F_N, A exhibits repetitive hysteretic loading or unloading cycles. These cycles are independent of the humidity, loading rates, and material contrast across the interface. This surprising behavior has a large effect on the system's frictional strength. Both these contact area dynamics and accompanying transient behavior will be explained by μm-scale slip of the contacting surfaces, which is induced by simple Poisson contraction or expansion of the elastic medium above the contact plane.

Our experimental apparatus is schematically described in Fig. 1(a), and detailed in [10,11]. The contact area of the slider block, made of poly-methyl-methacrylate (PMMA), is first diamond machined to an optical flatness and then polished to roughnesses ranging from 0.1–15 μm rms. Normal loads of $270\ \mathrm{N} < F_N < 5000\ \mathrm{N}$ are uniformly imposed via a compliant spring array sandwiched between two thick plates. The lower block (base) was either optically flat PMMA or BK7 glass, polished to a 100 nm rms roughness, or unpolished (smooth) float glass. Prior to each set of experiments all contact surfaces were first washed with a commercial detergent, and then cleaned with iso-

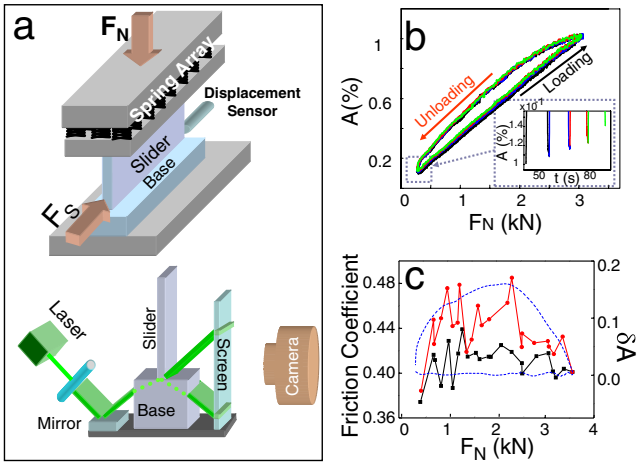

FIG. 1 (color online). (a) A schematic view of the experimental system. (top) Transparent slider and base blocks are loaded through a soft 40-spring array. Displacement is measured at both the leading and trailing edges (where F_S is applied) of the slider. (bottom) A laser sheet illuminates the interface though the base. Both the transmitted and reflected beams are imaged onto a fast camera. (b) The actual area of contact, A (in % of nominal contact area), vs F_N for 4 successive loading or unloading cycles. The samples were not separated between cycles and a minimum load of 270 N was retained. (inset) A, as a function of time at the lowest values of F_N, shows negligible contact area accumulation between consecutive cycles. (c) Static friction coefficient, μ_s directly measured upon loading (■) and unloading (●) over an F_N cycle, as in (b). The dashed line indicates the difference in contact area between loading and unloading, δA, as derived from (b). In (b) and (c) the slider and base were of PMMA, with a nominal contact area of 150×6 mm.

propyl alcohol and air dried. Shear force, F_S, when used, was applied to the trailing edge of the slider, as described in [10,11]. Displacements of both the slider's leading and trailing edges were measured to better than 10 nm resolution (Philtec D170 and D20 sensors).

Quantitative measurements of A were performed, as in [10,11] by illuminating the contact area with a laser sheet whose incident angle was well beyond the angle of total internal reflection for the base-air interface. If not illuminating a point of contact, the incident light decayed exponentially with a 50 nm decay length. The transmitted and reflected light are both imaged onto a high speed complimentary metal oxide semiconductor sensor having 1280 pixel resolution along the length of the interface. In this work we consider the overall change in A integrated over the entire interface. The transmitted intensity, I, normalized by the total incident intensity at each location, is, to a very good approximation, a linear function of A for small changes in F_N. Over large ranges of F_N the evanescently transmitted light induces [11] some curvature in $I(F_N)$. To obtain A, we normalized $I(F_N)$ by its initial values, $I_0(F_N)$, obtained for increasing loads over a range of F_N larger than used in subsequent measurements. $I_0(F_N)$ agrees with calculations of $I(A)$ [11], using a Gaussian distribution of contact points whose density and mean curvature are consistent with laboratory specimens. As the curvature of $I(F_N)$ is small, changes in I/I_0 will yield an excellent measure of corresponding changes in A.

We studied the change in the actual area of contact, A, with F_N for various loading protocols, with no external shear applied. Let us first consider the four typical successive loading or unloading cycles presented in Fig. 1(b). Significant hysteresis in each cycle is clearly visible, with nearly perfect reproducibility of the loading curves over the cycles. Less than 1% of the overall changes induced in A persist [inset of Fig. 1(b)] upon each unloading cycle.

Measurements [Fig. 1(c)] of the static coefficient of friction, $\mu_s = F_S/F_N$, show that, like A, there is a significant difference in μ_s for a *given* value of F_N, depending upon how one arrives at this value. The up to 15% increase in frictional strength roughly tracks the corresponding changes (up to 20%–25%) in A over the hysteretic cycle. As the measurements of A are much more accurate than those of μ_s it is difficult to say whether the differences in the two curves are significant. In this sense, measurement of A provides a more precise value for μ_s than can be obtained directly. Figure 1 also suggests that the large scatter that is generally obtained in measurements of μ_s may be largely due to these memory effects.

Scaling of the loading or unloading cycles is demonstrated in Fig. 2. Cycles with successively increasing maximal loads are shown in Fig. 2(a). Prior to the start of each cycle, we imposed large slip to erase any (small) memory effects induced by the previous cycle. Normalizing F_N by the range, ΔF_N, applied in each cycle collapses all data to a single curve [inset of Fig. 2(a)]. Similar scaling occurs [Fig. 2(b)] when the maximal load is fixed and the minimal values of F_N are successively decreased. In this experiment we did *not* impose slip between cycles and the system retains a memory of the maximum load or contact area attained [$A_{\max} \sim 4.5\%$ in Fig. 2(b)]. Upon reloading, the system targets this point. A collapse of the hysteresis contours, similar to the inset of Fig. 2(a), is obtained [inset of Fig. 2(b)] by rotation of these contours to a common axis prior to normalization by ΔF_N.

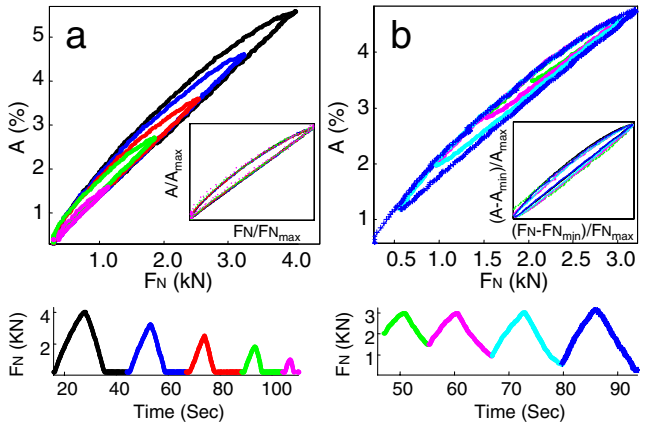

FIG. 2 (color online). A (in % of nominal contact area) as a function of F_N (top) and loading histories (bottom) in successive loading or unloading cycles for a PMMA/PMMA interface. (a) F_N is cycled from 270 N to decreasing maximal loads. Between cycles 1 mm slip was generated. inset of (a)—When F_N is normalized by ΔF_N, all curves collapse to a single curve. (b) The maximal F_N is fixed and successively lower minimal loads are applied. No slip was imposed between cycles and long-term memory is retained, as seen by the reloading curve axes orientation towards the maximal point achieved in the initial loading cycle. Here, [inset of (b)] data collapse upon normalization by ΔF_N occurs only after rotation to offset the axis orientation induced by long-term memory. Slider and base were of PMMA with a 30×6 mm nominal contact area.

Let us consider the form of the $A - F_N$ curves. As Fig. 3 demonstrates, these curves are independent of ambient humidity [7,9,12], material contrast across the interface, and loading rates. As we are in the regime [4,11] where $F_N/A = 400$ MPa $\sim \sigma_y$, plastic deformation at the PMMA contacts is predominant. The overall form of the $A - F_N$ curves may be understood in the framework of both plastic [3] or elastic-plastic [5,6] theories of contact deformation. Although adhesive processes [1] may play a role [13], we present a simple model, based on elastoplasticity, that accounts for both the form of the $A - F_N$ curves and their cyclic behavior [Fig. 1(b)].

Elastoplastic descriptions [3,5,6] of contact mechanics predict that the initial loading will deform the contact surface and cause hysteresis in A during unloading. This is, however, predicted to occur *solely* in the first loading cycle. Subsequent loading cycles are expected to retrace

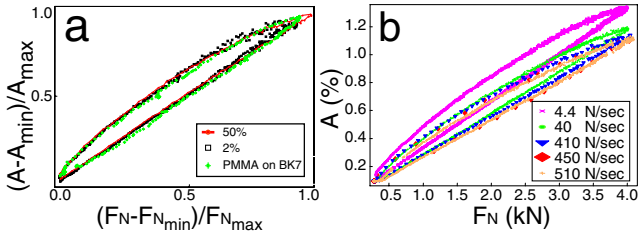

FIG. 3 (color online). A as a function of F_N is independent of humidity, material contrast, or viscoelasticity. (a) $A - F_N$ curves for a PMMA/PMMA interface at ambient humidities of 50% (line and squares) and 2% in dry nitrogen (circles) and (∇) a PMMA/BK7 interface (diamonds). Similar results where obtained for a silanated BK7 base. (b) $A - F_N$ curves for a PMMA/PMMA interface where loading rates were altered by over 2 orders of magnitude. Besides upward shifts due to aging, no apparent rate effects are observed.

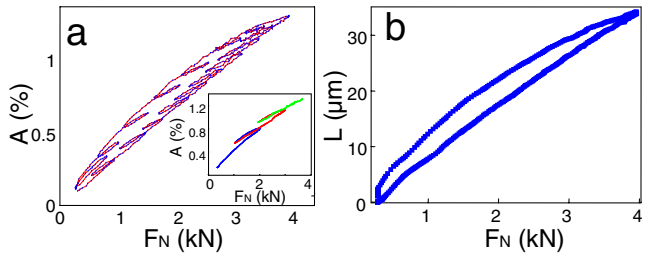

FIG. 4 (color online). Poisson effect and contact renewal. (a) Small amplitude (~400 N) oscillatory loading cycles, imposed on a full loading cycle yield negligible amounts of hysteresis for $F_N > 2500$ N, when the base material is PMMA. The inset shows that this region of negligible hysteresis is extended to a ~1200 N oscillation amplitude when using a base of float BK7 glass and roughened (~15 μm rms) PMMA slider. (b) Total slider expansion, ΔL, as a function of F_N during one loading or unloading cycle.

the unloading curve, as the contact deformation should not be significantly changed so long as the maximum value of F_N is not increased. If *renewal* of microcontacts were to occur between cycles, repetitive hysteretic cycles [as Fig. 1(b)] would occur. In a rough multicontact interface, effective contact renewal could occur via relative displacements of the interface that are larger than a single mean contact size. Such microscopic displacements could result from the differential motion due to Poisson expansion caused by application of purely normal loading. This will trivially occur in a dissimilar interface such as PMMA/BK7, but will also be evident in PMMA plates with different geometries and/or boundary conditions; e.g., our (thin) slider and much wider base that are, respectively, under effectively plane stress and plane strain conditions.

This model predicts that for sufficiently small cycles, where the maximum relative displacement is insufficient for contact renewal, hysteresis will disappear. For contact renewal to occur, however, the Poisson-induced shear, which is proportional to ΔF_N, must be large enough to induce local slip by overcoming the frictional forces, proportional to F_N, which pin the interface. Thus, Poisson-driven slip occurs above a critical value of $\Delta F_N/F_N$. This effect is demonstrated in Fig. 4(a), where small loading or unloading cycles are imposed on a large cycle by applying a small oscillatory component ($\Delta F_N \sim 400$ N) to F_N. Above $\Delta F_N/F_N \sim 0.2$ the hysteresis evident in the small cycles up to $F_N \sim 2500$ indeed disappears.

By replacing the base with an (unpolished) plate of float glass and a very rough (15 μm rms) slider, we can significantly extend the range of ΔF_N over which the hysteresis disappears [inset of Fig. 4(a)]. This occurs because the float glass surface is extremely smooth (<50 nm rms roughness) over scales much larger than PMMA asperity sizes. These surfaces then model an ideal smooth-rough interface [5], which, due to the translational invariance of the smooth surface, does not allow effective contact renewal [8] despite the increased Poisson effect due to the PMMA/glass mismatch. This result is not likely to be attributed to adhesion along the interface, and therefore supports the elastic-plastic model presented earlier.

Further support for this mechanism is obtained by direct measurements of the Poisson expansion, ΔL, of the slider as a function of F_N, as presented in Fig. 4(b). ΔL, measured by displacement sensors at opposing slider edges, closely echoes the hysteretic cycle of the $A - F_N$ measurements. Significantly, the total expansion is less than half of that calculated for frictionless boundary conditions. This indicates that changes in F_N generate residual shear stresses that are held in check by local friction of the microcontacts along the interface. It is, therefore, reasonable to assume that this local friction gives rise to the hysteretic behavior of A; motion leading to contact renewal is prevented with the pinned contacts' aging rates actually enhanced due to the residual shear stress [8]. Note that these results are obtained for a PMMA/PMMA interface with no ostensible material mismatch.

The interrelation of A and ΔL is further explored in Fig. 5. As demonstrated in Fig. 5(a), ΔL changes slowly with time. At a constant value of F_N, ΔL will, in general, increase slowly with time [Fig. 5(a), upper inset]. This continuous creep allows the system to slowly relax the Poisson-driven shear stress along the interface, which is opposed by the effective friction caused by interactions between the microcontacts across the surface. This "glassy" behavior of the contacts also occurs when F_N is suddenly reduced [Fig. 5(a), lower inset]. The corresponding decrease in ΔL is not immediate. Sliding, with a rate that continuously decreases with time, occurs until the shear stresses are, once again, balanced by microcontact interactions. Surprisingly, as shown in Fig. 5(b), ΔA is nearly *proportional* to ΔL. This is true when ΔL both increases and decreases in time, in both cases with the same constant of proportionality. Aging, the increase in A with time at a constant load, is a well-known phenomenon

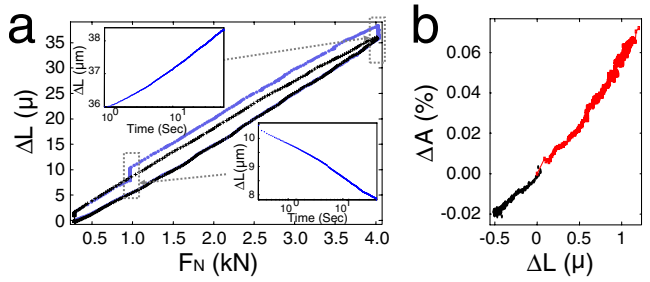

FIG. 5 (color online). Aging and de-aging of the system. (a) Measurement of slider expansion, ΔL, for two consecutive loading cycles where in the second cycle (circles) the load was held at 4000 N upon loading, and 1000 N upon unloading. Increase at 4000 N (upper inset) and *decrease* at 1000 N (lower inset) of slider length with time. The decrease is observed subsequent to a rapid reduction of F_N and continues until arriving at the steady-state (cross) curve. (b) Change in A (% of nominal contact area) as a function of ΔL where the normal load was held at $F_N = 2000$ N during loading (light line) and at $F_N = 1500$ N during unloading (dark line). The nearly linear dependence demonstrates both the strong coupling between ΔL and A and the equivalence of the increase in ΔL with aging and decrease with de-aging.

which is generally considered a consequence of the plastic flow of microcontacts. ''De-aging'', or the slow *decrease* in A shown in Fig. 5, commonly occurs in our experiments, when F_N is abruptly reduced. Unlike aging, which persists for extremely long times [7], de-aging levels off after a time that depends on the prior hold time. Strengthening then begins, with a logarithmic temporal growth in A whose rate (in PMMA/PMMA interfaces) is about half of the rate of change shown in Fig. 5(a). These competing processes are thus dominated by that with the highest rate, and the linear dependence of ΔA on ΔL [Fig. 5(b)] will disappear at longer time scales.

We have shown that, perhaps surprisingly, μm scale motion can exert a very large influence on the frictional properties of an interface. These effects, invisible using standard measurement techniques, were only observable by direct measurements of A over an entire interface. The strength of the Poisson expansion or contraction mechanism for contact surface renewal is in its generality. The microslip generated by this mechanism will cause contact renewal in any system in which individual microcontacts strengthen with their time of contact. Thus, any rough interface where time-dependent contact dynamics occur (e.g., plasticity and/or adhesion dominated) will be significantly affected.

The hysteretic effects described here are not accounted for in current theories of friction. As these microscopic motions produce large changes in the frictional properties of an interface, these effects should have a significant influence on the near critical behavior of frictional systems that are close to their threshold for motion. These include phenomena ranging from frictional motion at microscopic scales to the nucleation of earthquakes. For example, these effects may explain the large variation of measured coefficients of static friction (as the measurement protocol is important). They may also influence earthquake nucleation dynamics (where the preexistence of infinitesimal initial motion is a necessary condition of some current theories [14]) and suggest a new mechanism for triggering of new earthquakes via the stress changes generated by previous ones.

Enlightening conversations with J. L. Barrat, M. O. Robbins, and M. Urbakh helped to shape the course of this work. The authors acknowledge the support of the Israel Science Foundation (FIRST Grant No. 1116/05). J. F. received partial support of the National Science Foundation under Grant No. PHY99-0794.

[1] M. Urbakh, J. Klafter, D. Gourdon, and J. Israelachvili, Nature (London) **430**, 525 (2004).
[2] J. A. Greenwood and J. B. P. Williamson, Proc. R. Soc. A **295**, 300 (1966).
[3] F. P. Bowden and D. Tabor, *The Friction and Lubrication of Solids I* (Clarendon, Oxford, 1950); B. N. J. Persson, *Sliding Friction*, Nanoscience and Technology Series (Springer, Heidelberg, 1998).
[4] J. H. Dieterich and B. D. Kilgore, Pure Appl. Geophys. **143**, 283 (1994).
[5] L. Pei, S. Hyun, J. F. Molinari, M. O. Robbins, J. Mech. Phys. Solids (to be published).
[6] L. Kogut and I. Etsion, J. Appl. Mech. **69**, 657 (2002); J. Y. Kim, A. Baltazar, and S. I. Rokhlin, J. Mech. Phys. Solids **52**, 1911 (2004).
[7] J. H. Dieterich, J. Geophys. Res. **84**, 2161 (1979); T. Baumberger and C. Caroli, cond-mat/0506657.
[8] L. Bureau, T. Baumberger, and C. Caroli, Eur. Phys. J. E **8**, 331 (2002).
[9] J. Crassous, L. Bocquet, S. Ciliberto, and C. Laroche, Europhys. Lett. **47**, 562 (1999); L. Bocquet, E. Charlaix, S. Ciliberto, and J. Crassous, Nature (London) **396**, 735 (1998).
[10] S. M. Rubinstein, G. Cohen, and J. Fineberg, Nature (London) **430**, 1005 (2004).
[11] S. M. Rubinstein, M. Shay, G. Cohen, and J. Fineberg, cond-mat\0603528 [Int. J. Fract. (to be published)].
[12] K. M. Frye and C. Marone, J. Geophys. Res. **107**, 2309 (2002).
[13] Adhesion cannot be entirely ruled out here, since long range van der Waals forces would only be slightly affected by silanation, and the dipole interactions are similar for PMMA/PMMA and PMMA/glass interfaces.
[14] J. H. Dieterich and B. Kilgore, Proc. Natl. Acad. Sci. U.S.A. **93**, 3787 (1996).